Unified Fescription of Ucattering and Rropagation
FY13 Annual Report

David Paul Knobles
Applied Research Laboratories
The University of Texas at Austin
PO Box 8029
Austin, TX 78713
phone: (512) 835-3687   fax: (512) 835-3259
email: knobles@arlut.utexas.edu

LONG-TERM GOALS

The long-term goal of the research is to increase the physical understanding of acoustic propagation and scattering in continental shelf and slope environments in the 50-4000 Hz band. This includes both the physics of the seabed and the coupling to physical mechanisms in the water column in complex range- and azimuth-dependent littoral waveguides.

OBJECTIVES

For FY13, the first objective was to investigate the statistics of the mode intensity and cross-mode coherence that result from scattering from a randomly rough seabed surface in a shallow water environment. The second objective was to extract information about the frequency dependence of seabed attenuation for a soft thick sediment.

APPROACH

This research represents a collaborative effort between David Knobles and Dr. Jason Sagers, also with the Applied Research Laboratories, The University of Texas at Austin. The methods used to achieve the scientific goals and objectives are based on theoretical advances made over the previous two years. Two ideas in particular are unique to the analysis approach. For shallow water environments and acoustic frequencies below about 500 Hz, a coupled mode integral equation method that separates forward and backward propagating modal amplitudes in a physically consistent manner [1] is employed to investigate the statistics of propagation and scattering from a randomly rough seabed. For statistical inference of sediment attenuation dispersion, a maximum entropy method [2] is applied to newly recovered acoustic broadband data collected in the Gulf of Oman basin.

Report Documentation Page		Form Approved OMB No. 0704-0188

1. REPORT DATE **30 SEP 2013**	2. REPORT TYPE	3. DATES COVERED **00-00-2013 to 00-00-2013**
4. TITLE AND SUBTITLE **Unified Description of Scattering and Propagation FY13 Annual Report**		5a. CONTRACT NUMBER
		5b. GRANT NUMBER
		5c. PROGRAM ELEMENT NUMBER
6. AUTHOR(S)		5d. PROJECT NUMBER
		5e. TASK NUMBER
		5f. WORK UNIT NUMBER
7. PERFORMING ORGANIZATION NAME(S) AND ADDRESS(ES) **University of Texas at Austin,Applied Research Laboratories,Austin,TX,78758**		8. PERFORMING ORGANIZATION REPORT NUMBER
9. SPONSORING/MONITORING AGENCY NAME(S) AND ADDRESS(ES)		10. SPONSOR/MONITOR'S ACRONYM(S)
		11. SPONSOR/MONITOR'S REPORT NUMBER(S)

12. DISTRIBUTION/AVAILABILITY STATEMENT **Approved for public release; distribution unlimited**

13. SUPPLEMENTARY NOTES

14. ABSTRACT

15. SUBJECT TERMS

16. SECURITY CLASSIFICATION OF:			17. LIMITATION OF ABSTRACT	18. NUMBER OF PAGES	19a. NAME OF RESPONSIBLE PERSON
a. REPORT **unclassified**	b. ABSTRACT **unclassified**	c. THIS PAGE **unclassified**	**Same as Report (SAR)**	**9**	

Standard Form 298 (Rev. 8-98)
Prescribed by ANSI Std Z39-18

1. Statistics of propagation and scattering

The approach employed to examine the statistics of scattering and propagation, in a unified manner, utilizes an integral equation coupled mode method that was recently placed into a formulation that *splits* the modal amplitudes into *forward* and *backward* components. The critical aspect of the splitting is that the amplitudes are constrained to satisfy the appropriate asymptotic boundary conditions [1]. In contrast the backward component of the modal amplitudes in the COUPLED algorithm developed by Evans [3] does not satisfy the boundary condition (amplitude must be finite) at the origin in a cylindrical coordinate system. The appropriate boundary conditions depend on the choice of coordinate system.

The 2-D coupled mode equations of dimension $2N$ for the forward and backward modal amplitudes ($R^+(x) = [R_1^+, R_2^+, ..., R_{N-1}^+, R^+]$ and $R^-(x) = [R_1^-, R_2^-, ..., R_{N-1}^-, R_N^-]$) in Cartesian coordinates are

$$R_n^+(x) = \int_0^x G_n^+(x,x')S_n(x')dx' + \int_0^x G_n^+(x,x')\sum_{m=1}^N C_{nm}(x')R_m^+(x')dx' + \int_0^x G_n^+(x,x')\sum_{m=1}^N C_{nm}(x')R_m^-(x')dx'$$

$$R_n^-(r) = \int_x^\infty G_n^-(x,x')S_n(x')dx' + \int_x^\infty G_n^-(x,x')\sum_{m=1}^N C_{nm}(x')R_m^+(x')dx' + \int_x^\infty G_n^-(x,x')\sum_{m=1}^N C_{nm}(x')R_m^-(x')dx'$$

(1)

where S_n is the modal source function for the n*th* mode, C_{nm} is the mode coupling matrix operator, and N is the total number of modes. G_n^- and G_n^+ are the forward and backward propagating Green's functions that satisfy the appropriate asymptotic boundary conditions

The seabed possesses spatial inhomogeneities in the form of fine-scale interface roughness and volume fluctuations in the sound speed and density. Thus, a single ocean acoustic measurement (or prediction) of propagation and scattering should be treated as a sample from an ensemble of possible acoustic field microstates. Then, like many other areas of physics, the meaningful quantities of interest become averages of physical quantities over an ensemble of sample measurements or predictions. Random realizations of the seabed roughness are generated from a roughness power spectrum. For each realization Eq. (1) is solved for $R_n^+(r)$ and $R_n^-(r)$. Then, the ensemble averages of the modal intensities $<|R_n^+|^2>$ and $<|R_n^-|^2>$, and the cross-mode coherences $< R_n^+(R_m^+)^* >$, $< R_n^-(R_m^-)^* >$, and $< R_n^+(R_m^-)^* >$ are computed for a sufficient sample size.

2. Maximum entropy based approach to statistical inference

A statistical inference approach seeks to answer the question, "Given data D what information can be inferred about model parameters M"? A Bayesian approach is a well-defined method to answer this question. A likelihood function is constructed and Bayes's formula then yields a posterior probability distribution (PPD) from which the information content for various model parameters are quantified. The key step is the construction of the likelihood. In this step it is necessary to make prior assumptions about the statistics of data-model errors. In Ref. 2 a maximum entropy (ME) approach was introduced that also computes a PPD. However, instead of first constructing a likelihood and using Bayess' rule, the PPD is directly obtained in the form of a canonical distribution, the most conservative distribution possible. No prior assumptions are made about the distribution of model and data errors. Rather, the canonical distribution becomes unique once certain constraints on the average error are specified. Reference 2 introduced a method where the constraint values can be estimated when there exist a

sufficient number of data samples that form an ensemble. This idea of data ensembles is consistent with the concept of computing/measuring ensemble averages of acoustic fields in the ocean.

The data currently being analyzed are well suited for the ME approach as a result of a large number of data samples and its analysis could potentially provide useful information on the seabed attenuation dispersion. The data were taken in the Gulf of Oman basin in the form of received time series signals generated by SUS explosions along a 200 km track. The physics that drives the information part of the process is that the received signals are composed of arrivals that have refracted within the body of the sediment. The approach attempts to obtain marginal distributions for the sound speed ratio and a gradient, assuming nominal attenuation values. Once parameter values are established that adequately predict the arrival time structure of the various refracting multipaths, the statistics of the frequency dependent attenuation are then established.

WORK COMPLETED

The work completed in FY13 includes the application of the split integral equation coupled mode methodology to quantify the ensemble-averaged modal intensity and cross-mode coherence for a case of strong (Born series does not converge) seabed scattering. Also, preliminary results have been obtained for the frequency dependence of the attenuation for a soft seabed sediment using data collected in the Gulf of Oman. A manuscript is in preparation for the application of ME to obtain the sound speed structure of the sediment.

RESULTS

1. Statistics of the mode intensity and cross-mode coherence

The effect of seabed roughness on the modal intensities and cross-mode coherence as a function of range was examined for a shallow water waveguide [4]. The background waveguide is 50 m deep with a stratified sound speed profile (SSP) over a half-space. The half-space sound speed and density are 1645 m/s and 1.9 g/cm^3, respectively. The SSP was one measured during the SW06 experiment and has a thermocline depth at about 20 m. The roughness wavenumber power spectrum employed to generate a 1-D rough seabed realization is

$$P(k) = \frac{K_L h^2}{\pi (K_L^2 + k^2)^{\gamma/2}},$$

(2)

where h, K_L, γ, and k are the rms roughness height, the roll-off wavenumber given by the reciprocal of the roughness correlation length, the scattering exponent, and the spatial wavenumber, respectively. Values selected for γ, K_L, and h in Eq. 2 were 2.0, 0.1 m^{-1}, and 0.25 m, respectively. These parameters generate realizations that are consistent with a very rough seabed surface classification. The roughness realizations were then superimposed onto the 50 m flat bathymetry. For the computations in this study the depth of the waveguide was set to its background value for $x < x_a$ and $x > x_b$, with x_a and x_b set to 1000 and 9000 m, respectively. Computations were made with the seabed attenuation set to 0.0 for the purpose of testing the prediction of modal equipartition assuming that $<|R_n^+|^2>$ and $<|R_n^-|^2>$ satisfied a *master* equation [5-6]. Also, computations were made for a seabed attenuation set to 0.4 dB/λ for the purpose of testing the effect of the ensemble-averaged modal intensities and cross-mode coherence to a typical attenuation for a sand sediment.
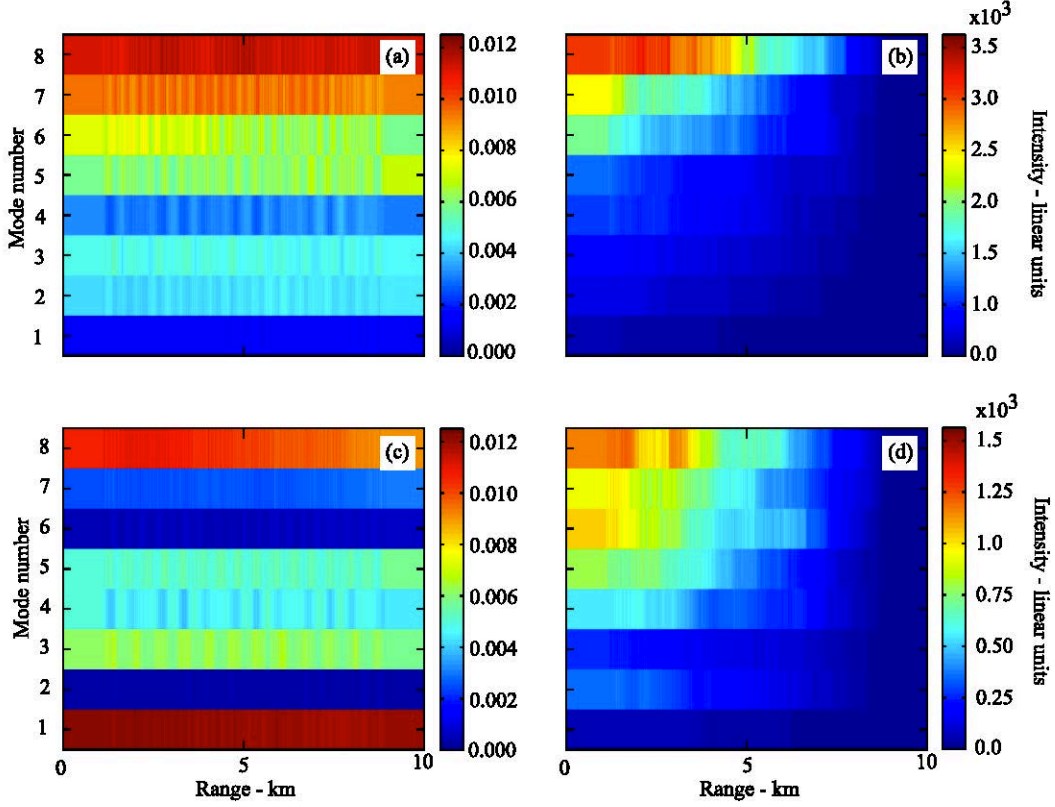
FIGURE 1. Ensemble-averaged modal intensities for zero attenuation case: (a) forward component 50 m source depth, (b) backward component 50 m source depth, (c) forward component 38 m source depth, and (d) backward component 38 m source depth.

Figure 1 shows $<|R_n^+|^2>$ and $<|R_n^-|^2>$ for the zero-attenuation case. The acoustic frequency is 300 Hz. While $<|R_n^+|^2>$ does not have the high variability observed for a single realization, it does possess a complex structure on both small and large spatial scales. Generally, even though there is significant modal scattering from for $x_a < x < x_b$ the asymptotic ($x > x_b$) modal intensity distributions do not exhibit equipartition for either the 50 m and the 38 m source depth case as would be predicted by a solution to a *master* equation without attenuation [5-6]. Rather, the asymptotic distribution for the forward propagating modes is strongly influenced by the initial distribution of mode intensity at $x=0$.

Figure 2 shows $<|R_n^+|^2>$ and $<|R_n^-|^2>$ for the non-zero attenuation case. The addition of attenuation changes the nature of the modal evolution with range in a profound manner since the propagation provided by G^+ is damped as a result of attenuation given by the imaginary part of the horizontal wavenumber eigenvalues; $<|R_n^+|^2>$ has the characteristic feature of a decrease in mode intensity with increasing x and mode number. This is a *mode stripping* effect. The attenuation also causes $<|R_n^-|^2>$ to be substantially different from the zero attenuation case. As a result of the attenuation mode 8 no longer contains the largest portion of the backscattered field. While it is still true that $<|R_n^-|^2>$ will increase, albeit in a non-uniform manner, for decreasing x, the additional factor of attenuation causes peaks in $<|R_n^-|^2>$ for $x > 0$.
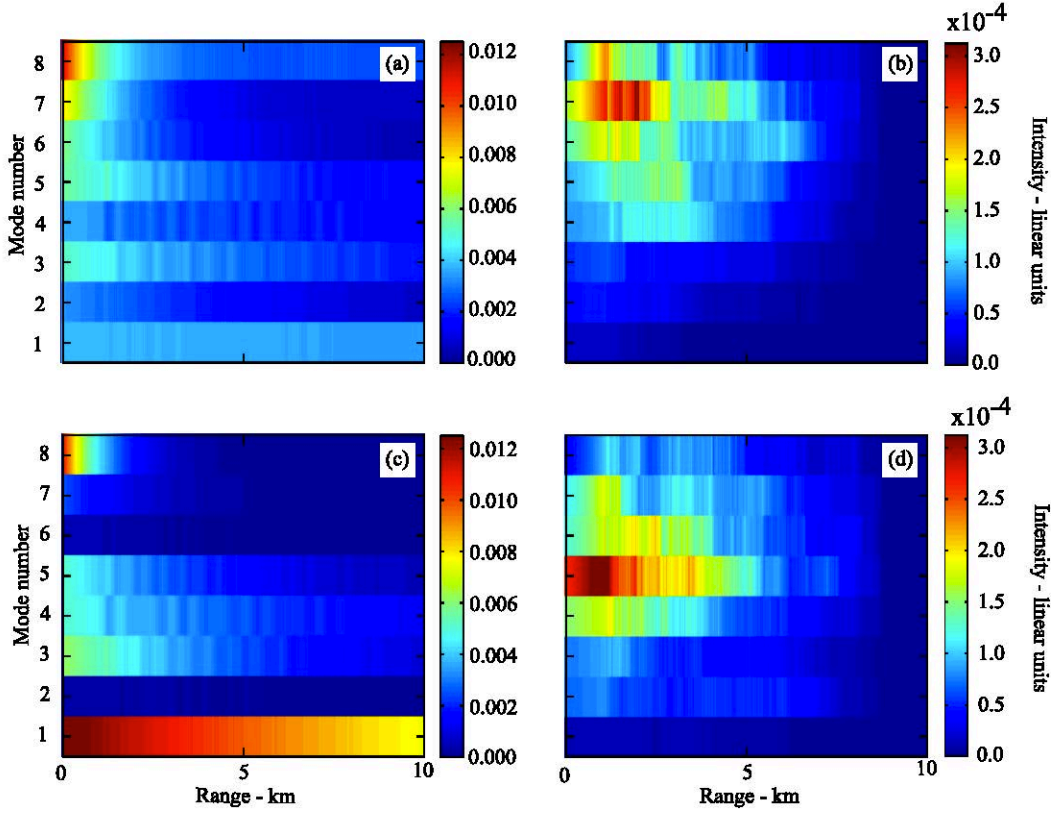
FIGURE 2. Ensemble-averaged modal intensities for non-zero attenuation case: (a) forward component 50 m source depth, (b) backward component 50 m source depth, (c) forward component 38 m source depth, and (d) backward component 38 m source depth.

Figure 3 shows $< R_n^+ (R_m^+)^* >$, $< R_n^- (R_m^-)^* >$, and $< R_n^+ (R_m^-)^* >$ for zero attenuation and the source depth at 50 m. The cross-mode coherences in Fig. 3 have been normalized such that they have values between 0 and unity. There are sixteen subpanels, each containing sixteen ensemble-averaged cross-mode coherence versus mode number and range. Overall, $< R_n^+ (R_m^+)^* >$ is near unity between 0 and 5 km and then decreases very slightly for ranges greater than 5 km. This observation is consistent with the observation in Fig. 1 that $<| R_n^+ |^2>$ does not show signs of equipartition. On the other hand $< R_n^- (R_m^-)^* >$ is significantly smaller than $< R_n^+ (R_m^+)^* >$ and the cross-coherence with range might be described as complicated. For $< R_n^+ (R_m^-)^* >$ coherence levels are about the same size as $< R_n^- (R_m^-)^* >$. However, much of the structure in the cross-mode coherence is independent of the *n*th modal index. This is evident in either the upper half of the first group of eight subpanels or the lower half of the second group of eight subpanels in Fig. 3.
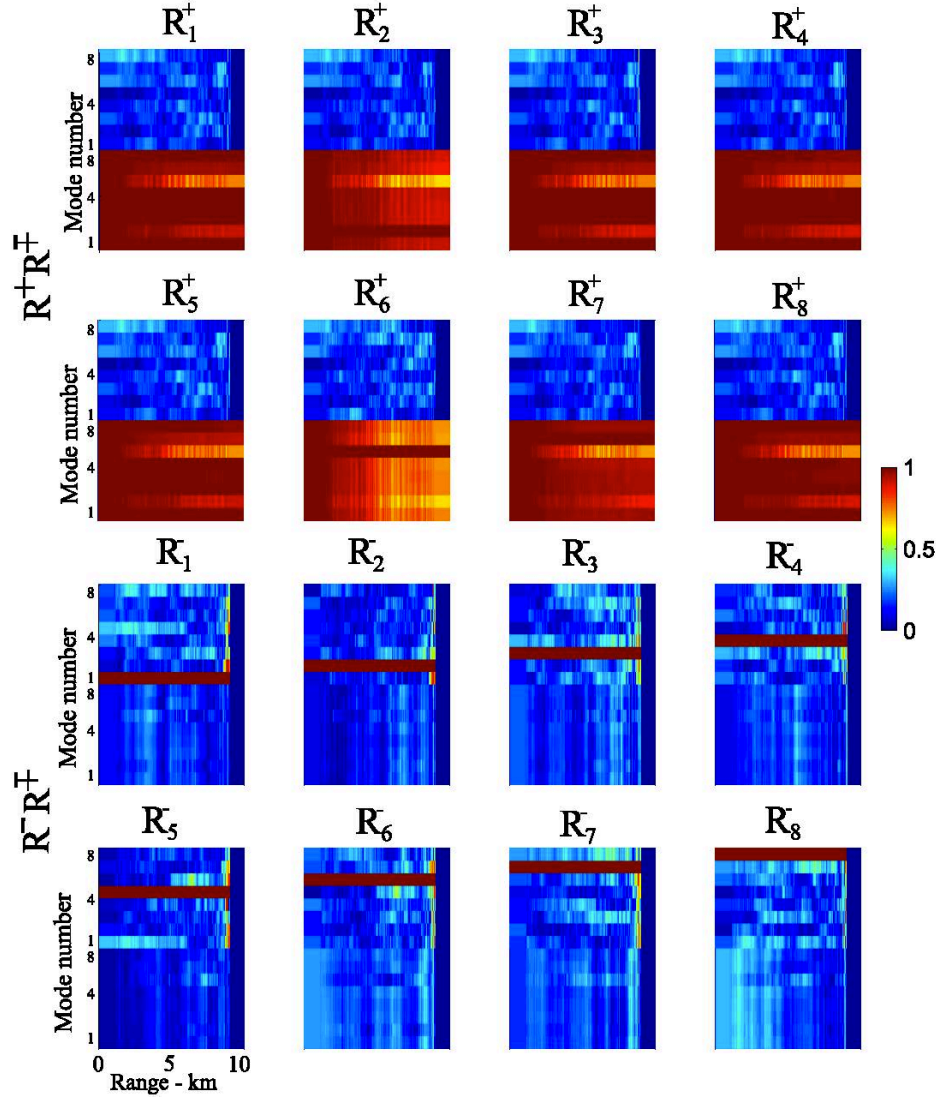
5

FIGURE 3. Ensemble-averaged modal cross-mode coherence for zero attenuation case with source depth of 50 m.

2. Frequency dependence of seabed attenuation in a soft thick seabed.

Addressed is the statistical inference of the sound speed depth profile and attenuation of a thick soft seabed from broadband sound propagation data recorded in the Gulf of Oman basin. The acoustic data are in the form of time series signals recorded in 1977 on a sparse vertical line array and generated by explosive sources deployed along a 250 km track. A maximum entropy (ME) method is employed to obtain marginal probability distributions for values of the sound speed ratio and the sound speed gradient. The specific types of data from which information about the sediment sound speed structure is inferred are those where most of the energy travels along sediment refracting paths. The ME analysis of the Gulf of Oman data reveals a range-dependence of the marginal distributions for the sound speed ratio and the gradient. There is no evidence for a non-linear depth profile. This range-dependence appears to be driven by an inherent parameter ambiguity between the ratio and the gradient.

This analysis is incomplete; however, a preliminary result is shown here. A more complete discussion will be provided in Ref. 7.
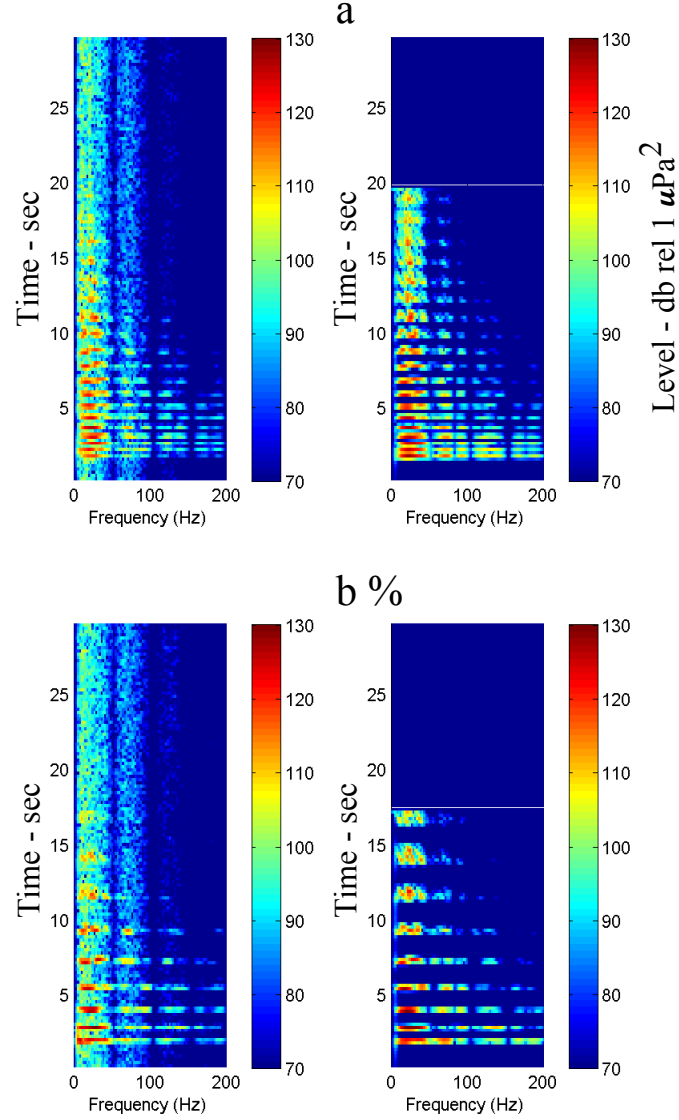
FIGURE 4. Modal (right) and data (left) comparisons of spectrograms of received acoustic intensity for a source-receiver range of about 99 km: (a) 1685 m receiver depth and (b) 3321 m receiver depth. Source depth is 88 m.

Figure 4 shows a model-data comparison of a spectrogram of the received time series in a 200 Hz band. The signal is characterized by multiple arrivals. An increase in the arrival number corresponds to an increase in the number of bottom interactions or equivalently the grazing angle of the refracted raypaths increase with increasing time of arrival. Thus, the later the arrival time the greater depth into the sediment that the acoustic field penetrates. The mean sound speed ratio is 1.008 and the sound speed gradient is about 1.62 1/s. Hamilton and Bachman previously reported values of about 0.99 and 1.3 1/s for the ratio and gradient, respectively, using high angle 2-way travel time reflection data measured on sonobuoys [8]. The attenuation is assumed to have the form of

$$A(f) = \alpha(f/1000)^n \tag{4}$$

where f is in Hz and α is in dB/m @ 1 kHz. $A(f)$ has units of dB/m.

The earliest arrival saturated the data recording on the magnetic tape, and thus appears at a lower level than in the modeled arrival. However, the agreement between the model and the data for the remainder of the arrivals appears fairly good up to about 15 seconds where the signal to noise ratio of the data becomes too small. The values used for α and n in Fig. 4 were 0.038 dB/m @ 1 kHz and 1.15, respectively. At this early point in the analysis, the difference of the exponent from unity is too small to view the dispersion to be different from linear. The statistical analysis of the attenuation is currently underway.

IMPACT/APPLICATIONS

One potential impact of this research is that these studies may assist in understanding how to optimally combine advanced propagation models and information inference methods as one proceeds to study ocean waveguides with increasing complexity and inhomogeneity. The issue of mode coherence is of direct importance to understanding sonar.

TRANSITIONS

The combined studies of statistical inference and the statistical effects of seabed scattering are expected to relate propagation statistics to physical mechanisms on continental shelf and slope environments.

RELATED PROJECTS

Related research projects include applying maximum entropy to issues in passive sonar.

REFERENCES

1. D. P. Knobles and J. D. Sagers, "A nonlocal effective operator for coupling forward and backward propagating modes in inhomogeneous media," J. Acoust. Soc. Am. **130** 2673-2680 (2011).
2. D. P. Knobles, J. D. Sagers, and R. A. Koch, "Maximum entropy approach for statistical inference in an ocean acoustic waveguide," J. Acoust. Soc. Am. **131** 1087-1101 (2012).
3. R. Evans, "The decoupling of stepwise coupled modes," J. Acoust. Soc. Am. **80**, 1414-1418 (1986).
4. D. P. Knobles and J. D. Sagers, "Forward and backward modal statistics for rough surface scattering in shallow water," submitted to Journal of Computational Acoustics, August 2013.
5. L. B. Dozier and F. D. Tappert, "Statistics of normal mode amplitudes in a random ocean. I. Theory," J. Acoust. Soc. Am. **63** 353-365 (1978).
6. J. A. Colosi and A. K. Morozov, "Statistics of normal mode amplitudes in an ocean with random sound speed perturbations: Cross-mode coherence and mean intensity," J. Acoust. Soc. Am. **126** 1026-1035 (2009).
7. J. D. Sagers and D. P. Knobles, "Statistical inference of seabed sound speed structure in Gulf of Oman basin," in preparation for the Journal of Acoustical Society of America.
8. E. L. Hamilton and R. T. Bachman, "Geoacoustic models of the sea floor: Gulf of Oman, Arabian Sea, and Somali Basin," Technical Report 357, Naval Ocean Systems Center (1978).

PUBLICATIONS

1. D. P. Knobles and J. D. Sagers, "Forward and backward modal statistics for rough surface scattering in shallow water," undergoing peer review in Journal of Computational Acoustics, August 2013.

2. D. P. Knobles, "The effect of surface roughness on the inference of frequency dispersion of seabed attenuation," in Advances in Ocean Acoustics: *Proceedings of the 3rd International Conference on Ocean Acoustics (OA2012)*, Beijing, China, AIP Conference Proceedings edited by Jixun Zhou, Zhenglin Li, and Jeffrey Simmen, Melville, New York 2012. Publication Date: December 17, 2012.

3. N. Ross Chapman and D. P. Knobles, "Perspectives on geoacoustic inversion," in Advances in Ocean Acoustics: *Proceedings of the 3rd International Conference on Ocean Acoustics (OA2012)*, Beijing, China, AIP Conference Proceedings edited by Jixun Zhou, Zhenglin Li, and Jeffrey Simmen, Melville, New York 2012. Publication Date: December 17, 2012.